Measurement of the Solar Neutrino Energy Spectrum Using Neutrino-Electron Scattering

Y. Fukuda,[1] T. Hayakawa,[1] E. Ichihara,[1] K. Inoue,[1] K. Ishihara,[1] H. Ishino,[1] Y. Itow,[1] T. Kajita,[1] J. Kameda,[1] S. Kasuga,[1] K. Kobayashi,[1] Y. Kobayashi,[1] Y. Koshio,[1] M. Miura,[1] M. Nakahata,[1] S. Nakayama,[1] A. Okada,[1] K. Okumura,[1] N. Sakurai,[1] M. Shiozawa,[1] Y. Suzuki,[1] Y. Takeuchi,[1] Y .Totsuka,[1] S. Yamada,[1] M. Earl,[2] A. Habig,[2] E. Kearns,[2] M. D. Messier,[2] K. Scholberg,[2] J. L. Stone,[2] L. R. Sulak,[2] C.W. Walter,[2] M. Goldhaber,[3] T. Barszczak,[4] D. Casper,[4] W. Gajewski,[4] P. G. Halverson,[4,*] J. Hsu,[4] W. R. Kropp,[4] L. R. Price,[4] F. Reines,[4,†] M. Smy,[4] H. W. Sobel,[4] M. R. Vagins,[4] K. S. Ganezer,[5] W. E. Keig,[5] R. W. Ellsworth,[6] S. Tasaka,[7] J. W. Flanagan,[8,‡] A. Kibayashi,[8] J. G. Learned,[8] S. Matsuno,[8] V. J. Stenger,[8] D. Takemori,[8] T. Ishii,[9] J. Kanzaki,[9] T. Kobayashi,[9] S. Mine,[9] K. Nakamura,[9] K. Nishikawa,[9] Y. Oyama,[9] A. Sakai,[9] M. Sakuda,[9] O. Sasaki,[9] S. Echigo,[10] M. Kohama,[10] A. T. Suzuki,[10] T. J. Haines,[11,4] E. Blaufuss,[12] B. K. Kim,[12] R. Sanford,[12] R.[1]Svoboda,[12] M. L. Chen,[13] Z. Conner,[13,§] J. A. Goodman,[13] G. W. Sullivan,[13] J. Hill,[14] C. K. Jung,[14] K. Martens,[14] C. Mauger,[14] C. McGrew,[14] E. Sharkey,[14] B. Viren,[14] C. Yanagisawa,[14] W. Doki,[15] K. Miyano,[15] H. Okazawa,[15] C. Saji,[15] M. Takahata,[15] Y. Nagashima,[16] M. Takita,[16] T. Yamaguchi,[16] M. Yoshida,[16] S. B. Kim,[17] M. Etoh,[18] K. Fujita,[18] A. Hasegawa,[18] T. Hasegawa,[18] S. Hatakeyama,[18] T. Iwamoto,[18] M. Koga,[18] T. Maruyama,[18] H. Ogawa,[18] J. Shirai,[18] A. Suzuki,[18] F. Tsushima,[18] M. Koshiba,[19] M. Nemoto,[20] K. Nishijima,[20] T. Futagami,[21] Y. Hayato,[21] Y. Kanaya,[21] K. Kaneyuki,[21] Y. Watanabe,[21] D. Kielczewska,[22,4] R. A. Doyle,[23] J. S. George,[23,‖] A. L. Stachyra,[23] L. L. Wai,[23,¶] R. J. Wilkes,[23] and K. K. Young[23,†]

(Super-Kamiokande Collaboration)

[1]*Institute for Cosmic Ray Research, University of Tokyo, Tanashi, Tokyo 188-8502, Japan*
[2]*Department of Physics, Boston University, Boston, Massachusetts 02215*
[3]*Physics Department, Brookhaven National Laboratory, Upton, New York 11973*
[4]*Department of Physics and Astronomy, University of California, Irvine, Irvine, California 92697-4575*
[5]*Department of Physics, California State University, Dominguez Hills, Carson, California 90747*
[6]*Department of Physics, George Mason University, Fairfax, Virginia 22030*
[7]*Department of Physics, Gifu University, Gifu, Gifu 501-1193, Japan*
[8]*Department of Physics and Astronomy, University of Hawaii, Honolulu, Hawaii 96822*
[9]*Institute of Particle and Nuclear Studies, High Energy Accelerator Research Organization (KEK), Tsukuba, Ibaraki 305-0801, Japan*
[10]*Department of Physics, Kobe University, Kobe, Hyogo 657-8501, Japan*
[11]*Physics Division, P-23, Los Alamos National Laboratory, Los Alamos, New Mexico 87544*
[12]*Department of Physics and Astronomy, Louisiana State University, Baton Rouge, Louisiana 70803*
[13]*Department of Physics, University of Maryland, College Park, Maryland 20742*
[14]*Department of Physics and Astronomy, State University of New York, Stony Brook, New York 11794-3800*
[15]*Department of Physics, Niigata University, Niigata, Niigata 950-2181, Japan*
[16]*Department of Physics, Osaka University, Toyonaka, Osaka 560-0043, Japan*
[17]*Department of Physics, Seoul National University, Seoul 151-742, Korea*
[18]*Department of Physics, Tohoku University, Sendai, Miyagi 980-8578, Japan*
[19]*The University of Tokyo, Tokyo 113-0033, Japan*
[20]*Department of Physics, Tokai University, Hiratsuka, Kanagawa 259-1292, Japan*
[21]*Department of Physics, Tokyo Institute of Technology, Meguro, Tokyo 152-8551, Japan*
[22]*Institute of Experimental Physics, Warsaw University, 00-681 Warsaw, Poland*
[23]*Department of Physics, University of Washington, Seattle, Washington 98195-1560*

(Received 8 December 1998)

A measurement of the energy spectrum of recoil electrons from solar neutrino scattering in the Super-Kamiokande detector is presented. The results shown here were obtained from 504 days of data taken between 31 May 1996 and 25 March 1998. The shape of the measured spectrum is compared with the expectation for solar ^{8}B neutrinos. The comparison takes into account both kinematic and detector related effects in the measurement process. The spectral shape comparison between the observation and the expectation gives a χ^2 of 25.3 with 15 degrees of freedom, corresponding to a 4.6% confidence level. [S0031-9007(99)08700-1]

PACS numbers: 26.65.+t, 14.60.Pq, 95.85.Ry, 96.40.Tv

Previous solar neutrino experiments [1–5] have measured significantly smaller neutrino flux than the expectation from standard solar models (SSMs) [6–9], an enigma that has been known as "the solar neutrino problem" for almost three decades. Detailed studies of this discrepancy between the observations and predictions strongly suggest that the apparent deficits in the measured fluxes are not easily explained by modifying the solar models, but can be

 0031-9007/99/82(12)/2430(5)$15.00

naturally explained by neutrino oscillations [10]. Since the expected spectral shape of the solar neutrinos can be calculated using well-established results from the terrestrial experiments, measurement of the solar neutrino energy spectrum can provide a direct, solar model-independent test of the neutrino oscillation hypothesis. ^{8}B solar neutrinos are detected in the Super-Kamiokande detector by observing recoil electrons resulting from neutrino-electron scattering in the water. The observed energy spectrum of recoil electrons reflects that of the ^{8}B solar neutrinos arriving on Earth.

In a previous letter, we reported a measurement that confirmed the solar ^{8}B neutrino flux deficit by utilizing the first 300 days of data [5]. The updated measured flux using 504 days of data is $2.44 \pm 0.05(\text{stat})^{+0.09}_{-0.07}(\text{syst}) \times 10^6\ \text{cm}^{-2}\,\text{s}^{-1}$, which corresponds to a ratio data/SSM of $0.474^{+0.010\,+0.017}_{-0.009\,-0.014}$, using the latest calculation by Bahcall *et al.* (BP98) [6], and $0.506^{+0.011\,+0.018}_{-0.010\,-0.015}$, using Brun *et al.* [9]. In this Letter we present a measurement of the recoil electron energy spectrum based upon 504 live days of data collected with the Super-Kamiokande detector.

Super-Kamiokande, a 50 000 ton imaging water Cherenkov detector, utilizes a 22 500 ton fiducial volume for the solar neutrino analysis; details of the detector are described in Ref. [5]. The vertex position and direction of the recoil electrons are reconstructed by using the timing information and ring pattern of the hit photomultiplier tubes (PMTs) [5]. Vertex position and angular resolutions for 10 MeV electrons are 0.71 m and 26.7°, respectively. Electron energy is measured by calculating the effective number of hit PMTs, N_{eff}, which is the number of hit PMTs with corrections for light attenuation through the water, the angular dependence of PMT acceptance, the effective density of PMTs, the number of nonfunctioning PMTs, and the probability of a two-photoelectron emission in one PMT. The N_{eff} corrections are designed to remove position and water transparency related effects so as to give uniform response over the fiducial volume.

Precision energy calibration of the detector is essential for the energy spectrum measurement of recoil electrons. We employ an energy calibration procedure using an electron linear accelerator (LINAC) to relate N_{eff} to absolute energy. The absolute energy scale is monitored for stability and cross-checked using the following: (1) muon decay electrons, (2) spallation products induced by cosmic ray muons, (3) ^{16}N produced by stopping muon capture on oxygen, and (4) a Ni(n, γ)Ni source.

The LINAC is used for calibrating the absolute energy scale and also for measuring the angular and vertex position resolutions. Details of the LINAC calibration are described in [11]. The uncertainty in the beam energy deposition in the Super-Kamiokande detector is 0.55% at 6 MeV and 0.3% at 10 MeV, resulting from the uncertainty in the beam energy ($<$20 keV) and the reflectivity of the beam pipe end-cap materials. Energy calibration utilizes LINAC data taken at eight representative positions within the Super-Kamiokande fiducial volume with seven different momenta ranging from 4.89 to 16.09 MeV. The absolute energy scale, the relation between N_{eff} and the total electron energy, is obtained from a Monte Carlo (MC) simulation program for which various parameters are tuned to reproduce the LINAC data taken at the various positions and energies. The MC simulation is based on GEANT 3.21 with the water attenuation lengths (absorption and scattering lengths) and reflectivity of detector materials, such as the light barrier surfaces separating the inner and outer detectors and the surfaces of 50 cm PMTs, as tunable parameters. After tuning, the MC simulation reproduces the position dependence of the energy scale as measured by the LINAC to within 0.5% on average. The energy resolution for electrons is also calibrated by the LINAC, and the difference between LINAC data and the corresponding MC simulation is less than 2%. Figure 1 shows the measured energy spectrum of LINAC 10.78 MeV data compared with the corresponding MC simulation. There is good agreement in the shape over 2 orders of magnitude, demonstrating that the MC simulation accurately translates input electron energy into energy measured by the detector.

The large number of muon decay electrons, $\sim$1500 events/day, allows monitoring of the temporal variation of water attenuation length. The variation of the water attenuation length has caused $\sim$3.8% change in the energy scale over the data taking period considered in this paper. After correcting N_{eff} for the variations in water attenuation length, the stability of the energy scale

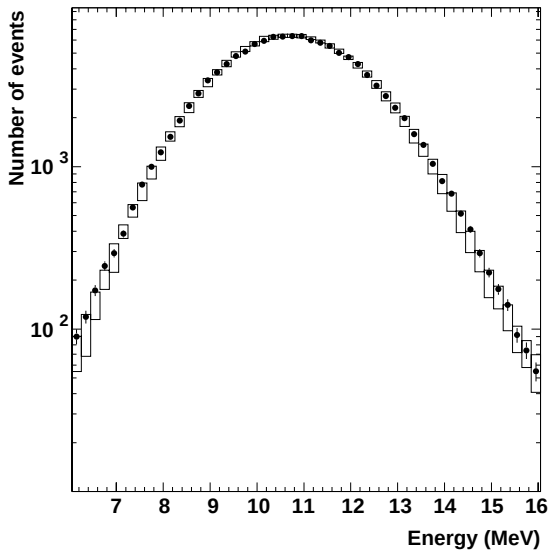

FIG. 1. The measured energy spectrum of 10.78 MeV LINAC electrons is shown by the data points. The data points are the sum of the values taken at eight representative positions within the detector. The boxes are the summation of values from the corresponding MC simulations, where the vertical size of a box indicates the estimated systematic errors in energy scale and resolution added in quadrature with statistical error.

is better than 0.5% over the time period described here and ~0.2% in rms. This variation is included in the uncertainty in the absolute energy scale, since the energy scale set by the LINAC calibration is extrapolated to the entire time period of this analysis.

The directional dependence of the energy scale was cross-checked using spallation events, which are beta and gamma rays from radioactive nuclei created by cosmic ray interactions within the detector. The spallation events are subdivided into ten data sets according to the reconstructed zenith angle and the relative difference of the energy distribution among the ten data sets is compared. The obtained angular dependence of the energy scale is less than 0.5%. This result allows the use of the LINAC absolute energy calibration, which thus far has been taken with electrons moving only in the downward-going direction, for all directions.

Another cross-check on the absolute energy calibration is made using the decays of ^{16}N produced by stopping muon capture on oxygen. These events with well-defined decay lines are also uniformly distributed in time and position, thus, providing another natural handle on absolute energy calibration. The difference in energy scales between that obtained by ^{16}N decay beta spectrum and the MC tuned to LINAC data is $0.2^{+0.6}_{-0.8}\%$.

Summing all possible sources of the uncertainty in the absolute energy scale described above in quadrature, the overall uncertainty in the energy scale is estimated to be $\pm 0.8\%$ at 10 MeV, which includes contributions from the uncertainty in the LINAC electron energy deposition ($\pm 0.3\%$), the position dependence of the energy scale ($\pm 0.5\%$), the uncertainty of the water transparency determination ($\pm 0.2\%$), and the directional dependence of the energy scale ($\pm 0.5\%$).

The energy dependence of the angular resolution of the detector is measured by using LINAC data [11]. The measured angular resolution is (2–3)% smaller than the corresponding MC simulation. The difference could be due to an inaccurate description of light scattering in the current MC simulation, but it is not yet fully understood. This difference in the angular resolution is corrected for in the solar neutrino flux calculation which follows.

For the energy spectrum measurement analysis, we follow the same data reduction procedure described in Ref. [5]. We have used the data obtained from 504 live days between 31 May 1996 and 25 March 1998. The data set (initially consisting of $\sim 7 \times 10^8$ events) was reduced by requiring that event vertices be within the fiducial volume and by instituting cuts designed to reject external gamma ray and muon-induced spallation events. The total efficiency of the data reduction is $(70.0 \pm 0.7)\%$ [5].

The final data sample is subdivided into 16 energy bins, every 0.5 MeV from 6.5 to 14.0 MeV and 1 bin combining events with energies from 14.0 to 20.0 MeV. The number of solar neutrino events in each energy bin is extracted individually by analyzing the angular distribution of the events within each bin with respect to the sun. The angular distribution in the region far from the solar direction provides a measure of the background level. A near-isotropic background angular distribution with respect to the direction of the sun is obtained with small corrections made for slight directional anisotropies in local detector coordinates. The background fit, along with the expected angular distributions of the solar neutrino signal, is incorporated into a maximum likelihood method to extract the number of solar neutrino events. The error in the number of solar neutrino events due to possible local detector anisotropies using this technique is 0.1%. The number of solar neutrino events thus obtained is shown in Fig. 2. The measured spectrum is then compared with the expected spectrum obtained from our MC simulation. The MC events are generated using (1) the total ^{8}B solar neutrino flux from Ref. [6] (5.15×10^6 cm^{-2} s^{-1}; a particular SSM is not required for the spectral shape analysis), (2) the calculation of ^{8}B neutrino spectral shape from Ref. [12], and (3) the electron spectrum of ν-e scattering from Ref. [13], in which radiative corrections are taken into account. The smearing of the expected recoil electron energy spectrum, mainly by the finite energy resolution of the detector, is done by a full detector simulation. The simulated MC events are then passed through the same analysis chain as the data, resulting in a MC recoil energy spectrum shown as a histogram in Fig. 2. In order to compare the shape of the observed energy spectrum with the expectation, the ratio of observed and expected numbers of events for each energy bin is taken; these ratios are plotted in Fig. 3.

Systematic errors in the energy shape comparison are classified into three categories: (1) energy-bin-correlated

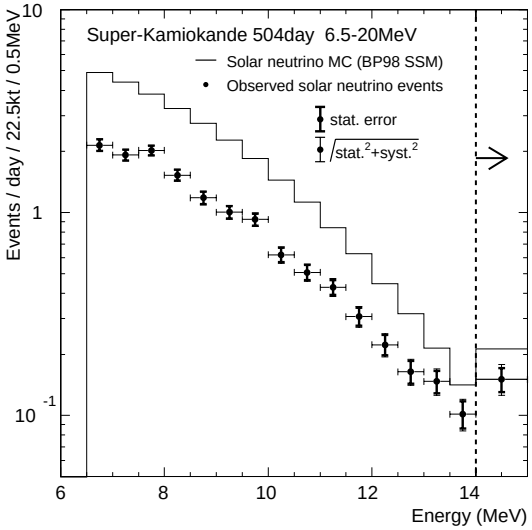

FIG. 2. Recoil electron energy spectrum of solar neutrinos (data points). The histogram shows the expectation from the SSM. The inner and outer error bars show the statistical and systematic errors, respectively. The systematic error is the sum of correlated experimental and calculation errors and uncorrelated errors added quadratically.

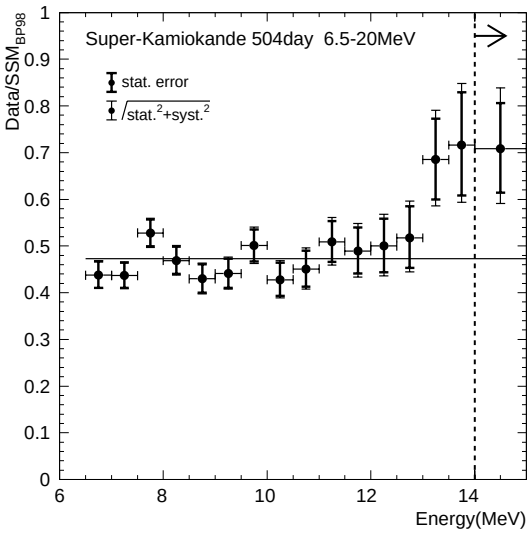

FIG. 3. Ratio of observed electron energy spectrum and expectation from the SSM. Errors are the same as in Fig. 2.

experimental errors (called "correlated" from now on), (2) energy-bin-correlated error in the expected energy spectrum calculation, and (3) energy-bin-uncorrelated ("uncorrelated") errors. The sources of correlated experimental errors are uncertainties in the absolute energy scale and energy resolution. The systematic error of the electron energy spectrum due to the correlated experimental uncertainties is shown in Table I. For example, the systematic error of the 13.0 to 13.5 MeV energy bin is $^{+6.9}_{-6.2}\%$, in which $^{+6.6}_{-5.9}\%$ comes from the uncertainty of the absolute energy scale and $^{+2.2}_{-1.9}\%$ from the uncertainty of the energy resolution. The correlated error in the expected spectrum calculation is obtained by using the 1σ error of ^{8}B neutrino energy spectrum described in Ref. [12] and shown in Table I. The sources of uncorrelated errors are the uncertainty in trigger efficiency (+1.2% error in energy spectrum only for 6.5–7.0 MeV energy bin), the uncertainty in the data reduction efficiency ($\pm 0.7\%$), the uncertainty in the directional anisotropy of the background ($\pm 0.1\%$), and the uncertainty in the size of the fiducial volume by possible systematic shift of the vertex position ($\pm 1.0\%$). Uncertainties which may be energy-bin-correlated, but whose energy dependence is not well known, are categorized as uncorrelated systematic errors by assigning the largest possible deviation in the energy spectrum to each energy bin. Such errors include the uncertainty in angular resolution ($\pm 1.0\%$) and the uncertainty in the cross section of ν-e scattering ($\pm 0.5\%$). The sum of uncorrelated errors is shown in Table I.

TABLE I. 1σ error of the flux due to correlated experimental error (second column), due to calculation of the expected spectrum (third column), and due to uncorrelated systematic error (fourth column).

Energy (MeV)	$\delta_{i,\text{exp}}$	$\delta_{i,\text{cal}}$	$\delta_{i,\text{uncorrelated}}$
6.5–7.0	$^{+1.3}_{-1.2}\%$	$^{+0.5}_{-0.1}\%$	$^{+2.1}_{-1.7}\%$
7.0–7.5	$\pm 1.3\%$	$^{+0.6}_{-0.3}\%$	$\pm 1.7\%$
7.5–8.0	$\pm 1.5\%$	$^{+0.8}_{-0.5}\%$	$\pm 1.7\%$
8.0–8.5	$\pm 1.8\%$	$^{+1.0}_{-0.7}\%$	$\pm 1.7\%$
8.5–9.0	$^{+2.1}_{-2.2}\%$	$^{+1.2}_{-1.0}\%$	$\pm 1.7\%$
9.0–9.5	$\pm 2.5\%$	$^{+1.5}_{-1.2}\%$	$\pm 1.7\%$
9.5–10.0	$\pm 2.9\%$	$^{+1.8}_{-1.5}\%$	$\pm 1.7\%$
10.0–10.5	$\pm 3.3\%$	$^{+2.1}_{-1.8}\%$	$\pm 1.7\%$
10.5–11.0	$^{+3.8}_{-3.7}\%$	$^{+2.4}_{-2.1}\%$	$\pm 1.7\%$
11.0–11.5	$^{+4.3}_{-4.2}\%$	$^{+2.8}_{-2.4}\%$	$\pm 1.7\%$
11.5–12.0	$^{+4.9}_{-4.6}\%$	$^{+3.2}_{-2.7}\%$	$\pm 1.7\%$
12.0–12.5	$^{+5.5}_{-5.1}\%$	$^{+3.7}_{-3.0}\%$	$\pm 1.7\%$
12.5–13.0	$^{+6.2}_{-5.7}\%$	$^{+4.2}_{-3.4}\%$	$\pm 1.7\%$
13.0–13.5	$^{+6.9}_{-6.2}\%$	$^{+4.7}_{-3.8}\%$	$\pm 1.7\%$
13.5–14.0	$^{+7.7}_{-6.8}\%$	$^{+5.2}_{-4.1}\%$	$\pm 1.7\%$
14.0–20.0	$^{+9.9}_{-8.5}\%$	$^{+6.7}_{-5.2}\%$	$\pm 1.7\%$

The observed energy spectrum is examined using the following χ^2:

$$\chi^2 = \sum_{i=1}^{16} \left\{ \frac{(\frac{\text{data}}{\text{SSM}})_i - \alpha/[(1 + \delta_{i,\text{exp}} \times \beta)(1 + \delta_{i,\text{cal}} \times \gamma)]}{\sigma_i} \right\}^2 + \beta^2 + \gamma^2,$$

where $\delta_{i,\text{exp}}$ and $\delta_{i,\text{cal}}$ are 1σ errors of the correlated experimental error and of the expected spectrum calculation described above, σ_i is a 1σ error for each energy bin defined as a sum of statistical error and uncorrelated errors added quadratically, and α is a free parameter which normalizes the measured ^{8}B solar neutrino flux relative to the expected flux. β and γ are parameters used for constraining the variation of correlated systematic errors. The minimum value of this χ^2 is obtained by numerically varying the parameters α, β, and γ, which results in a minimum value of 25.3 (with 15 degrees of freedom), a value of α of 0.449, and values of β and γ (measured in standard deviations) of -1.49 and -0.93, respectively. The resulting minimum χ^2 corresponds to an agreement of the measured energy shape with the expected energy shape at the 4.6% confidence level. The rather poor fit of χ^2 is due mainly to the rise in the observed spectrum at the high-energy end, where the uncertainties in the absolute energy scale and resolution can have large effects. To account for the rise with these uncertainties, the absolute energy scale must be shifted, horizontally, by 3.6% or the energy resolution worsened by 20%. These values are 4 and 10 times larger than the estimated uncertainties, respectively. Hence, the rise in the spectrum is difficult to explain with these experimental uncertainties.

The contribution of high energy solar neutrinos from $^3\mathrm{He} + p \rightarrow {}^4\mathrm{He} + e^+ + \nu_e$ (hep) is estimated using the best estimate flux in the SSM [6], $2.1 \times 10^3\ \mathrm{cm}^{-2}\mathrm{s}^{-1}$. The expected number of events during the 504 live day period is 0.84 and 1.3 events for energy ranges of 13–14 MeV and 14–20 MeV, respectively. The uncertainty in the SSM calculation of the hep neutrino flux is not precisely known, but an explanation of the high-energy points in terms of a hep neutrino component would require a dramatic increase in the SSM expectation.

In conclusion, we have measured the recoil electron energy spectrum from ^{8}B solar neutrinos with the Super-Kamiokande detector. A comparison of the observed spectrum with the expectation exhibits poor agreement at the 4.6% confidence level. An interpretation in terms of neutrino oscillations will be published later.

We gratefully acknowledge the cooperation of the Kamioka Mining and Smelting Company. This work was partly supported by the Japanese Ministry of Education, Science and Culture and the U.S. Department of Energy.

*Present address: NASA, JPL, Pasadena, CA 91109.
†Deceased.
‡Present address: Accelerator Laboratory, High Energy Accelerator Research Organization (KEK), Tsukuba, Ibaraki 305-0801, Japan.
§Present address: Enrico Fermi Institute, University of Chicago, Chicago, IL 60637.
‖Present address: California Institute of Technology, Pasadena, CA 91125.
¶Present address: Department of Physics, Stanford University, CA 94305.

[1] B. T. Cleveland *et al.*, Nucl. Phys. (Proc. Suppl.) **B38**, 47 (1995); R. Davis, Prog. Part. Nucl. Phys. **32**, 13 (1994).
[2] K. S .Hirata *et al.*, Phys. Rev. Lett. **65**, 1297 (1990); K. S. Hirata *et al.*, Phys. Rev. D **44**, 2241 (1991); **45**, 2170E (1992); Y. Fukuda *et al.*, Phys. Rev. Lett. **77**, 1683 (1996).
[3] J. N. Abdurashitov *et al.*, Phys. Lett. B **328**, 234 (1994).
[4] P. Anselmann *et al.*, Phys. Lett. B **327**, 377 (1994); **342**, 440 (1995).
[5] Y. Fukuda *et al.*, Phys. Rev. Lett. **81**, 1158 (1998).
[6] J. N. Bahcall, S. Basu, and M. Pinsonneault, Phys. Lett. B **433**, 1 (1998).
[7] J. N. Bahcall and M. Pinsonneault, Rev. Mod. Phys. **67**, 781 (1995).
[8] S. Turck-Chièze and I. Lopes, Astrophys. J. **408**, 347 (1993).
[9] A. S. Brun, S. Turck-Chièze, and P. Morel, Astrophys. J. **506**, 913 (1998).
[10] L. Wolfenstein, Phys. Rev. D **17**, 2369 (1978); S. M. Bilenky and B. Pontecorvo, Phys. Rep. **41**, 225 (1978); V. Barger, R. J. N. Phillips, and K. Whisnant, Phys. Rev. D **24**, 538 (1981); S. P. Mikheyev and A. Y. Smirnov, Sov. J. Nucl. Phys. **42**, 913 (1985).
[11] M. Nakahata *et al.*, Nucl. Instrum. Methods Phys. Res., Sect. A **421**, 113 (1999).
[12] J. N. Bahcall *et al.*, Phys. Rev. C **54**, 411 (1996).
[13] J. N. Bahcall *et al.*, Phys. Rev. D **51**, 6146 (1995).